LANGMUIR-BLODGETT NANOTEMPLATE CRYSTALLIZATION COMBINED TO LASER-MICROFRAGMENTATION UNIQUELY CHARACTERIZE PROTEINS CRYSTALS BY SYNCHROTRON MICRODIFFRACTION

[1,2,3]**Claudio Nicolini,** [1]**Luca Belmonte,** [3]**Christian Riekel,**
[4]**Christian Koenig and** [1,2]**Eugenia Pechkova**

[1]Laboratories of Nanobiotechnology and Biophysics,
University of Genova, Corso Europa 30, Genova, 6132, Italy
[2]Nanoworld Institute, Fondazione ELBA Nicolini, Pradalunga, Bergamo, 24029, Italy
[3]Experiments Division, European Synchrotron Radiation Facility, B.P.220, Grenoble Cedex, 38043, France
[4]Paul Scherrer Institute (PSI), Villigen, 5232, Switzerland

ABSTRACT

Laser-induced microfragmentation of LB nanotemplate-induced protein crystals in glycerol solution results in distinct, coherently diffracting domains. Only crystals produced according to the Langmuir-Blodgett (LB) nanotemplate technique reveal in all four proteins being tested (lysozyme, insulin, thaumatin and ribonuclease) domains highly radiation resistant, while the crystals produced by the standard hanging drop crystallization method do not. Actually the very same laser exposure causes the disappearance of these "classical" protein crystals during the same time frame of 40 min needed for the laser cutting in all four proteins being tested. The microdiffraction of microcrystals prepered by the combination of Langmuir-Blodgett and Laser technologies proves that not only the Lysozyme survives the process, as shown recently by nanodifraction, but also all three other model proteins appear to behave similarly well, namely insulin, thaumatin and ribonuclease. The result confirms the emerging of a new biophysical technique uniquely usefull for synchrotron radiation studies based on small protein microcrystals uniquely radiation resistant when prepered by LB nanotemplate and subsequently fragmented by Laser.

Keywords: Langmuir-Blodgett (LB), Force Microscopy (AFM)

1. INTRODUCTION

Laser-microdissection have recently (Pechkova *et al.*, 2013; Pechkova and Nicolini, 2010) been successfully used to dissect Langmuir-Blodgett lysozyme crystals (Nicolini and Pechkova, 2006a; Pechkova *et al.*, 2004; 2007; 2009; Belmonte *et al.*, 2012) in order to obtain pieces of crystals of very small dimensions in conjuction with X-ray nanodiffraction techniques capable to overcome the very common problem of twinned, defect, aggregated and mosaic crystals.

Laser microfragmentation of lysozyme crystals prepered by Langmuir-Blodgett nanotemplate (needs however to be extended to other protein models, such as ribonuclease, thaumatin and insulin, all less robust than lysozyme and systematically compared with their classical counterparts (Nicolini and Pechkova, 2006b; Pechkova *et al.*, 2004; 2007; 2009; Belmonte *et al.*, 2012) laser dissected, in order to establish its significance and its

Corresponding Author: Claudio Nicolini, Laboratories of Nanobiotechnology and Biophysics,
University of Genova, Corso Europa 30, Genova, 6132, Italy

general extension to protein crystallography (Nave, 1999; Pechkova and Nicolini, 2004). This is thereby the main objective of this comunication.

Several demonstration experiments show that laser-microdissection techniques can also be applied to protein crystals (Pechkova *et al.*, 2013; Pechkova and Nicolini, 2010). We have used the term laser-microdissection for the cutting of a crystal by a laser beam into smaller pieces (Pechkova *et al.*, 2013) while microfragmentation is used for the separation of a microdissected crystal into smaller fragments due to effects such as cavitations at domain boundaries and solvent interpenetration.We will explore in this contribution the question whether protein crystals differing in perfection and X-ray radiation stability also differ in microdissection and microfragmentation behavior. Indeed, protein crystals grown by a Langmuir-Blodgett (LB) based method (called LB-crystals) are shown here to have a unique higher radiation stability than crystals provided by standard (e.g., hanging drop) crystallization techniques (called standard-crystals) in the wide range of four quite different proteins. Atomic Force Microscopy (AFM) suggests also differences in surface topologies for protein crystals grown according to the two methods (Santucci *et al.*, 2011).

2. MATERIALS AND METHODS

2.1. Protein Crystallization by LB nanotemplate

Utilizing an up-to-date crystallization technique (Nicolini and Pechkova, 2006a; Pechkova *et al.*, 2004) based on Langmuir-Blodgett nanotemplate (Nicolini, 1997), crystals of four different model proteins (lysozyme, thaumatin, insulin and ribonuclease) are obtained. These crystals grown by nanostructured template (Pechkova *et al.*, 2009) appear more radiation resistant than the classical ones, even in presence of a third-generation highly focused ID13 beamline at the European Synchrotron Radiation Facility. The electron density maps and the changes in parameters like total diffractive power, B-factor and pairwise R-factor have been discussed. Protein crystals, grown by LB nanotemplate based method, proved to be more radiation resistant compared to crystals grown by classical hanging drop method in terms of global and specific damage (Pechkova *et al.*, 2004; 2009; Belmonte *et al.*, 2012), both used to compare radiation damage as function of dose. As suggested earlier (Belmonte *et al.*, 2012), three metrics are used to monitor global damage for both kinds of crystals, namely total diffracting power of crystal, Isotropic B Factor and Pairwise R Factor. Other commonly used metrics of radiation damage like

mosaicity and cell volume increment were utilized even if sometimes non-predictable increase or a non-linear behavior could happen. Specific structural changes in protein exposed to high radiation dose appear to occur for these LB protein crystals with respect to the classical hanging drop crystals in reproducible way, i.e., water distribution (Pechkova *et al.*, 2012a) and in specific sites and bonds, i.e., glutamates and aspartates and for disulphide bonds. Highly ordered, well diffracting and radiation stable crystals were confirmed for several other proteins, such as human protein kinase CK2 (Pechkova *et al.*, 2003), Oxygen-Bound Hell's Gate Globin I (Pechkova *et al.*, 2012a) and other model proteins (i.e., thermolysin, ribonuclease, thaumatine and insulin),which confirm the significant radiation resistance earlier reported for LB Proteinase K (Pechkova *et al.*, 2009), LB Lysozyme (Nicolini and Pechkova, 2006b; Pechkova *et al.*, 2004; Pechkova and Nicolini, 2004) and LB human kinase (Pechkova *et al.*, 2003) crystals, despite occasional gloomy opinions to the contrary.

LB-nanofilms were generated by the Langmuir-Blodgett (LB) technique and its variation, a modified Langmuir-Schaeffer technique (LS). Typically protein was spread at the air-water interface of an in-house LB-through and immediately compressed with 70 cm min^{-1} to a surface pressure of about 20 mN m^{-1}. The protein monolayers were transferred from the water surface onto siliconized cover slips by touching the support in parallel to the surface according to the LS-technique at the pressure of 20 mN m^{-1}. These LB-nanofilms were used as crystallization templates (Nicolini, 1997; Pechkova *et al.*, 2012a; 2012b; 2003). Crystallization conditions for LB- and standard-crystals were both based on the hanging drop vapour diffusion method (Pechkova *et al.*, 2012b).

2.2. Laser-Microdissection and Microfragmentation

Experiments were performed using a Zeiss PALM laser-microdissection system with a laser wavelength of $\lambda = 355$nm and <2 ns pulses of 90 J each at 100 Hz (ZEISS, 2012). This corresponds for a ~4 µm^2 laser spot to a laser fluency of ~562 J/cm^2 and a flux density of ~4*10^{21} photons s^{-1} mm^{-2}. The laser beam was focused on the surface of the crystal avoiding thus shockwave induced crack formation. In order to allow in-situ observation and manipulation of cut crystals, we performed microdissection operations for all four proteins being utilized, both classical and LB, in an open aqueous solution drop rather than in a sample cell or in a flash-frozen cryoloop. The freely floating protein crystals and the convective flow induced by evaporation

did, however, not allow clear cuts. In addition, the evaporation resulted also in salt precipitation which limited the time available for sample manipulation. The movement of crystals and fragments could, however, be significantly reduced by electrostatically fixing them to a mica sheet and using a more viscous ~20% glycerol solution. This also reduces the evaporation rate and allows in principle subsequent cryocooling of the sample. This method enabled recording high quality optical images of the microdissection process and subsequent microfragmentation; based on this observation we pursued two parallel routes of investigation using both classical amd LB crystals, namely:

- For microcrystallographic characterization in the 5 μm beamsize (this manuscript) for the four chosen proteins we transfer crystal microfragments from the drop into a cryoloop for cryofreezing
- For nanocrystallographic characterization in the 0.4 μm beamsize (Pechkova *et al*., 2013) we cut crystals directly in a nylon cryoloop which was aligned in the laser-beam by a micromanipulator

While for Lysozyme was shown earlier (Pechkova and Nicolini, 2010), the LB microdissectected and microfragmented crystals from the three other model proteins (insulin, ribonuclease and thaumatin) are given in **Fig. 1 and 2**. The Thaumatine, Ribonuclease and Insulin crystals in the pictures represent microdissected LB fragments obtained in 20% Glycerol.

20% Glycerol solution (Pechkova *et al*., 2013; Pechkova and Nicolini, 2010) got several advantages over the other solutions tested before. First of all, the time for the manipulation is not limited due to the creation of salt crystals, as in a water solution. Additionally, the Protein Crystals don't float around as fast as in Water, but are free enough to move away from each other after a cut. Furthermore, the crystals are not being dissolved in the Glycerol Solution. The only disadvantage is the appearance of bubbles in the solution which will not disappear, due to the viscosity. Nevertheless, it's possible to cut small parts of a crystal and to store them for a long enough time to catch them with a loop or with kapton grid (**Fig. 1**).

We have catched the crystals also either with a nylon loop mounted to a piezoelectric micromanipulator or manually. The advantage over the manual fishing is, that our manipulator is very stable and precise. Nevertheless, manual fishing is sufficient for getting hold of the crystals (**Fig. 1 and 2**).

2.3. Synchrotron Radiation Experiments and Data Processing

We used the ID13 beamline at the ESRF-Grenoble (Riekel *et al*., 2009). Experiments were performed with a monochromatic wavelength of $\lambda = 0.09611$ nm, using a beam focused by crossed linear Fresnel lenses to about 5 μm spot with a flux of $7*10^{10}$ photons/s. A raster-scanning goniometer with integrated air-bearing rotation axis was used. Sample supports were attached by a magnetic base to the ID13 scanning goniometer and aligned normal to the beam by an on-axis Olympus microscope, which was calibrated to the beamline focal spot. Experiments were performed in transmission geometry at 100 K using an Oxford Cryoflow system. Diffraction data were collected using a MAR CCD 165 detector with 1024*1024 pixels at a sample-to-detector distance of 114.41 mm for a typical exposure time/pattern of 1 s. The raster-diffraction experiments were analyzed with the FIT2D program (www.esrf.fr/computing/scientific/FIT2D/).

For the microcrystallographic acquisition processing and refinement were carried out as previously described (Pechkova *et al*., 2009; Belmonte *et al*., 2012) and radiation damage computed (Garman, 2010). Spacegroup $P4_32_12$ was recognized by POINTLESS (Evans, 2006) and all data sets were processed in this spacegroup. Dataset scaling was performed using SCALA and Freerflag from the CCP4 software package (Bailey, 1994). In order to obtain significant statistics, data were processed at high resolution. According to the Matthews coefficient results (Kantardjieff and Rupp, 2003) molecular replacement was performed with only one molecule in the asymmetric unit assuming a protein mass of 14.3 KDa. Automated molecular replacement was performed using MOLREP (Vagin and Teplyakov, 1997) and the lysozyme structure derived from thin-film-based crystals (PDB 2AUB) (Pechkova *et al*., 2005) as template (Berman *et al*., 2003). The PDB file was then refined using REFMAC5 (Murshudov *et al*., 1999) for both datasets. Manipulation of PDB files was performed using RASMOL (Sayle, 1995). Before the final refinement step, electron density maps were inspected by COOT (Emsley *et al*., 2010) at the same contour level of 0.78e $Å^{-3}$ and a last refinement step was performed. Statistics of data collection, processing and refinement are shown in **Table 3**. Visual inspection of protein structures was performed using PyMol (2012).
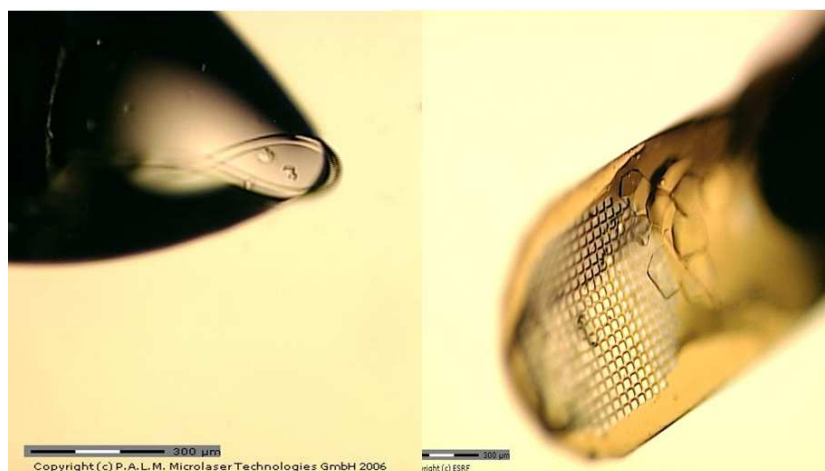
Fig. 1. Langmuir-Blodgett Protein Microcrystals obtained by laser microdiffracted, eiher of Insulin fished in the beamline loop (left) or of Ribonuclease captured in a Kapton grid (right)
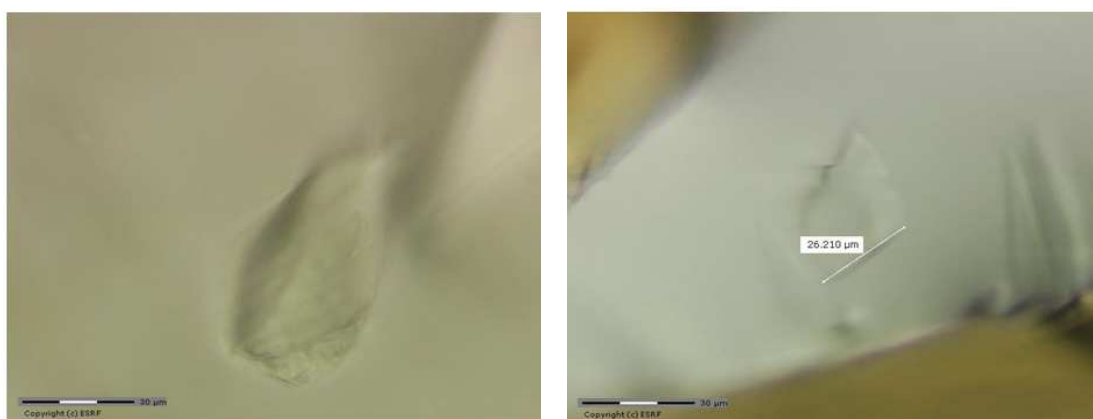

Fig. 2. _Laser Microfragments of Insulin (right) and Thaumatin (left) Microcrystals prepered by Langmuir-Blodgett nanotemplate

3. RESULTS AND DISCUSSION

3.1. Laser-Microfragmentation of Protein Crystals

Table 1 summarizes the crystallization conditions for all four different proteins under hanging drop vapour diffusion either with or without LB nanotemplate.

Numerous small microcrystals have then been produced by laser cutting only on LB crystals since the classical crystals completely disappears under the same laser exposure of 40 min. This allows to evaluate radiation damage (Garman, 2010) by synchrotron microfocussing on higly focussed ID13 beamline (5 microns beamsize) in these quite small crystals

obtained as shown in **Table 1 and 2** by using the same proteins utilized in the ID14/23/29 beamlines studies (Pechkova *et al.*, 2009; Belmonte *et al.*, 2012). Actually on the last proteins microcrystals we have applied additional continous laser expsosure which has quite larger number of photons per unit area and unit time with respect to synchrotron radiation beamlines. The laser cutting of microfragmentated crystals for all four proteins have been carried out for crystal size indicated in **Table 2** in Langmuir-Blodgett crystals by laser proper exposure for 40 min. The very same laser exposure of 40 min needed for the laser cutting of all four LB proteins being tested causes the disappearance of all "classically-prepered" protein crystals, namely for lysozyme, thaumatin, insulin and ribonuclease.

Table 1. Crystallization conditions at T=25^{0}C of LB-crystals used for laser microdissection

Protein	Protein solution	Reservoir	Drop
Lysozyme (from hen egg white)	40 mg mL^{-1} 50 mM sodium acetate pH 4.5	0.9 NaCl in 50 mM sodium acetate	1:1
Thaumatin (from Thaumatococcus Daniellii)	15 mg mL^{-1} in 100 mM ADD buffer pH 6.5	1 M Na/K tartrate in 100 mM ADD buffer pH 6.5	1:1
Insulin (from bovine pancreas)	18 mg mL^{-1} in 50 mM Na$_2$HPO$_4$ pH 10.4 1 mM EDTA	400 mM Na$_2$HPO$_4$ pH 10.4 10 mM EDTA	1:1
Ribonuclease	10 mg mL^{-1} in 50 mM Na-acetate pH 5.5	1.75 M (NH$_4$)$_2$ SO$_4$ 2 M NaCl in 100 mM Na-acetate pH 5.5	1:1

Table 2. LB-induced Protein Microcrystals obtained by Laser microdissection and microfragmentation

Protein	Crystal Size(micron^2)	Beamsize (Microns)	Number of Images per Dataset at 1° of rotation
Thaumatin	10×30	5	82
Insulin	10×26	5	90
Ribonuclease	30×22	5	122
Lysozyme	10×30	5	38

3.2. X-ray Microdiffraction of Microfragmented LB-Crystals

In the lst column of **Table 2** are indicated the number of diffraction images acquired from each protein microcrystals. According to the Matthews coefficient results molecular replacement was performed with only one molecule in the asymmetric unit assuming a protein mass of 14.3 KDa for Lysozyme, 22.22 KDa for Thaumatin, 5.733 KDa for Insulin and 13.7 KDa for Ribonuclease. Automated molecular replacement was performed using MOLREP (Vagin and Teplyakov, 1997) using PDB templates with the following Ids: 2AUB for Lysozyme, 4DJ0 for Thaumatin, 4I5Z for Insulin and 3I6F for Ribonuclease as template. The PDB files were then refined using REFMAC5 (Murshudov *et al.*, 1999) for all datasets. Before the final refinement step, electron density maps were inspected by COOT (Emsley *et al.*, 2010) at the same contour level. Statistics of data collection, processing and refinement are shown in **Table 1**. Absorbed dose calculation was performed using RADDOSE (Murray *et al.*, 2004) assuming beam energy of 12.9 KeV, λ = 0.0961Å, beamsize of 5×5 μm^2, exposure time of 1 s and a flux of about 7*1010 photons/s corresponding to a flux density of about 3*1011 ph/s/μm2, other parameters are shown in **Table 3**.

Image acquisition (**Fig. 4**) agrees with the minimum number of images needed for data completeness and symmetry, e.g., for a spacegroup P 41 21 2 (point group 422) found for thaumatin more

than 45 images were acquired. Despite to this latter sentence spacegroup recognition was difficult and not obvious in all the so far discussed laser-fragmented protein crystals with the microfocused beam. This is probably due to a very low number of diffraction patterns with a good number of high I/sigma spot. Anyway, even after laser cutting a lots of diffraction patterns could be still acquired and the very difficult solving task could be avoided with ad hoc techniques for microdissected crystals acquisition; indeed, as shown in **Fig. 3** excellent diffraction patterns were acquired for thaumatin and insulin, proving the principle of laser macrofragmentation in all four protein being studied.

The radiation dose and the comparable crystallographic parameters are computed for both synchrrotron and laser assuming beam flux density of 2×1013 photons μm-2 s-1 and Energy of 12.7 KeV. Dose calculation is made by the following equation:

$$D(Gray) = \mu E t I0$$

Where:

μ = Mass absorption coefficient (cm2/g)
E = Energy of the X-ray (KeV)
t = Time of exposure (seconds)
I0 = Flux of the X-ray beam (photons/s/nm2)

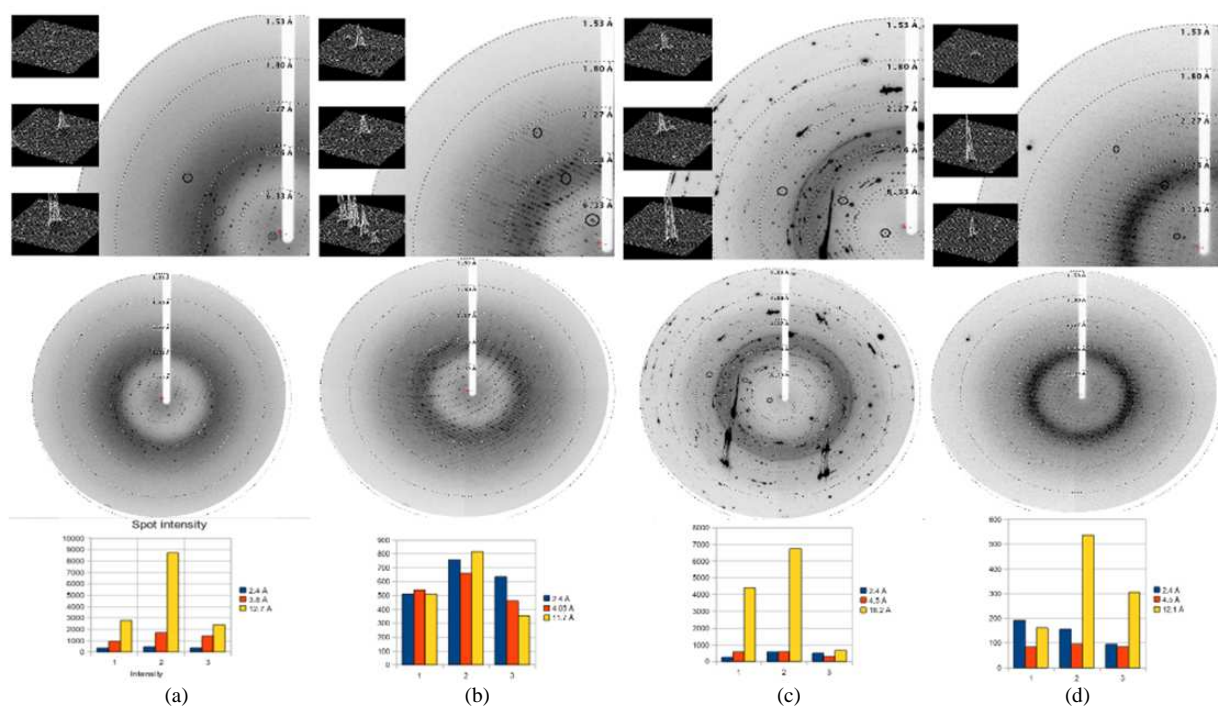The estimate of total dose was computed using the program RADDOSE (Murray *et al.*, 2004).

Fig. 3. Resolution rings (above) and their relative signal intensity of the reflection corresponding to identified different shell of progressive higher resolution (middle) for a diffraction pattern of laser microdissected insulin (a), thaumatin (b), ribonuclease (c) and lysozyme (d) crystals induced by LB nanotemplate vapour diffusion method; (below) Histogram of microcrystal spot intensity at 2.4, 3.8 and 12.7 Å resolution for Insulin LB (left), 2.4, 4.05 and 11.7 Å for thaumatin LB (center) 2.4, 4.5 and 16.2 Å for LB ribonuclease (right)
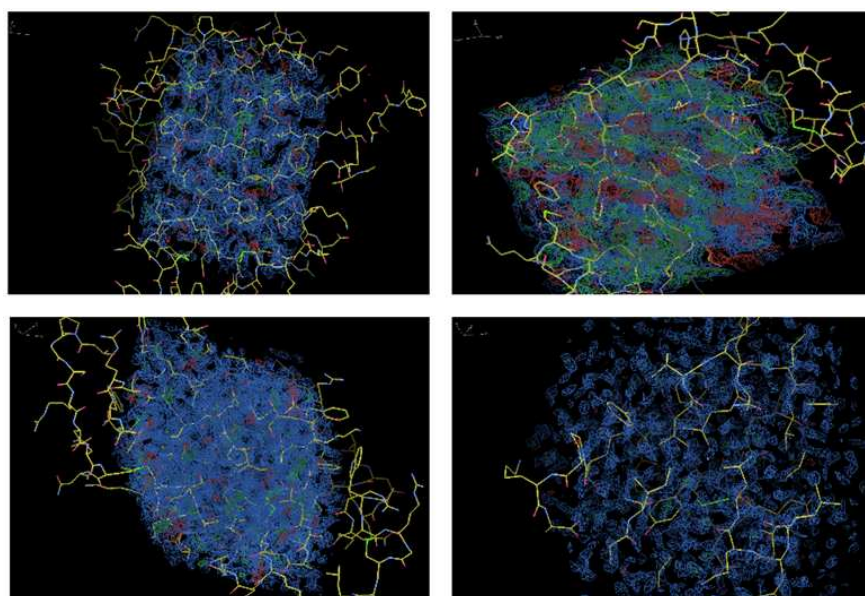

Fig. 4. Electron Density map from upper corner left clockwise Thaumatin, Ribonuclease, Insulin, Lysozyme microcrystals laser dissected. Statistics are shown in **Table 2**

Table 3. Statistics for microdissected LB crystals acquired with microfocus on ESRF ID13.

Parameters	Insulin	Thaumatin	Ribonuclease	Lysozyme
Resolution (Å)	1.39-18.26	1.98-45.34	2.37-48.92	1.57-38.29
Unit cell a,b,c (Å)	77.49 77.49 77.49	103.2, 103.2, 151.4	106.71, 116.31, 234.9	95.56 38.29 109.89
α, β, γ (°)	90 90 90	90 90 90	94.24, 98.05, 103.22	90 109.64 90
Spacegroup	I 21 3	P 41 21 2	P 1	P121
Mosaicity (°)	1.127	0.567	0.454	0.885
$R_{-factor}$	0.6	0.36	0.5	0.4
R_{free}	0.63	0.42	0.5	0.43
I/ σ	0.48	0.21	0.23	0.1
Completeness%	77.82	85.22	55.56	26.83
Total number of reflections	11629	46874	239805	26802
Mean B-value for side chains	2.0	2.0	2.0	2.0
R.m.s. on bond length (Å)	0.012	0.015	0.027	0.01
R.m.s. in bond angle (°)	1.543	1.640	2.652	1.449
N°of water mol	1213	1213	33	559

Table 4. Absorbed dose for microdissected crystals acquired with microfocus and nanofocus and for laser microdissected crystals

Protein crystal	Absorbed Dose (Gy) for laser microdissected crystals	Absorbed Dose (Gy) for microdissected crystals acquired with microfocus and nanofocus
Thaumatin	$0.331*10^{19}$	$0.668*10^{8}$
Ribonuclease	$0.52*10^{19}$	$0.108*10^{9}$
Insulin	$0.368*10^{19}$	$0.748*10^{8}$
Lysozyme	$0.141*10^{19}$	$0.272*10^{8}$

4. CONCLUSION

Results of radiation dose calculation are shown in **Table 4**, where it become readily apparent the enormous increase in the absorbed radiation dose with the laser-induced microdissection which explain the disappearance of "classical" protein crystals in all four cases and makes more striking the effect of LB nanotemplate in dramatically enhancing radiation stability. Radiation damage limits the highest resolution data collection on a single spot, as is indeed conclusively shown in a native globin protein crystal recently solved (Pechkova *et al*., 2012b) and in model proteins using submicron Grazing Incidence Small Angle Scattering (Pechkova and Nicolini, 2011; Pechkova *et al*., 2010; Gebhardt *et al*., 2010). Overall analysis indicates more damage suffered by the classical crystals than the LB ones. By taking into account what so far discussed, LB crystals confirm the greater radiation- resistance on both global and specific damage side (Belmonte *et al*., 2012; Pechkova *et al*., 2012a; Murshudov *et al*., 1999). The suggestion for a possible reason for the radiation resistance of the LB-based crystal has been raised recently (Pechkova *et al*., 2012a) in terms of the dehydration observed to lead to better ordered protein crystals and to the significantly improved diffraction limit (Heras *et al*., 2003; Kuo *et al*., 2003; Nicolini and Pechkova, 2006a).

A fundamental clue of the unique physical-chemical properties and features of Langmuir-Blodgett crystals derives from the very recent collection of sophisticated studies down to the nanoscale (Pechkova *et al*., 2013; Pechkova and Nicolini, 2010). However the main efforts of LB-based crystallization should be addressed in the future mainly to overcome the barriers in membrane protein structures determination still existing (Nicolini and Pechkova, 2006b) despite all gigantic efforts.

4.1. Supporting Material

The atomic coordinates and structural factors have been deposited in the Protein Data Bank (www.pdb.org). LB1: RCSB ID code is RCSB074134; PDB ID code 4GFZ; LB2: RCSB ID code is RCSB074135; PDB ID code 4GG0

5. AKNOWLEDGEMENT

6. REFERENCES

Bailey, S., 1994. The CCP4 suite: Programs for protein crystallography. Acta Cryst. D, 50: 760-763. DOI: 10.1107/S0907444994003112

Belmonte, L., E. Pechkova, S. Tripathi, D. Scudieri and C. Nicolini, 2012. Langmuir-blodgett nanotemplate and radiation resistance in protein crystals: State of the art. Crit. Rev. Eukaryot. Express., 22: 211-224. PMID: 23140163

Berman, H., K. Henrick and H. Nakamura, 2003. Announcing the worldwide protein data bank. Nat. Struct. Biol., 10: 980-980. DOI: 10.1038/nsb1203-980

Emsley, P., B. Lohkamp, W.G. Scott and K. Cowtan, 2010. Features and development of Coot. Acta Cryst. D, 66: 486-501. DOI: 10.1107/S0907444910007493

Evans, P., 2006. Scaling and assessment of data quality. Acta Cryst. D, 62: 72-82. DOI: 10.1107/S0907444905036693

Garman, E., 2010. Radiation damage in macromolecular crystallography: What is it and why should we care? Acta Cryst. D, 66: 339-351. PMID: 20382986

Gebhardt, R., E. Pechkova, C. Riekel and C. Nicolini, 2010. In Situ μGISAXS: II. Thaumatin crystal growth kinetic. Biophys. J., 99: 1262-1267. DOI: 10.1016/j.bpj.2010.03.068

Heras, B., M.A. Edeling, K.A. Byriel, A. Jones and S. Raina *et al.*, 2003. Dehydration converts DsbG crystal diffraction from low to high resolution. Structure, 11: 139-145. DOI: 10.1016/S0969-2126(03)00005-4

Kantardjieff, K.A. and B. Rupp, 2003. Matthews coefficient probabilities: Improved estimates for unit cell contents of proteins, DNA and protein-nucleic acid complex crystals. Protein Sci., 12: 1865-1871. DOI: 10.1110/ps.0350503

Kuo, A., M.W. Bowler, J. Zimmer, J.F. Antcliff and D.A. Doyle, 2003. Increasing the diffraction limit and internal order of a membrane protein crystal by dehydration. J. Struct. Biol., 141: 97-102. DOI: 10.1016/S1047-8477(02)00633-0

Murray, J.W., E.F. Garman and R.B.G. Ravelli, 2004. X-ray absorption by macromolecular crystals: The effects of wavelength and crystal composition on absorbed dose. J. Applied Cryst., 37: 513-22. DOI: 10.1107/S0021889804010660

Murshudov, G.N., A.A. Vagin, A. Lebedev, K.S. Wilson and E.J. Dodson, 1999. Efficient anisotropic refinement of macromolecular structures using FFT. Acta Cryst. D, 55: 247-255. DOI: 10.1107/S090744499801405X

Nave, C., 1999. Matching X-ray source, optics and detectors to protein crystallography requirements. Acta Cryst. D, 55: 1663-1668. DOI: 10.1107/S0907444999008380

Nicolini, C. and E. Pechkova, 2006a. Nanostructured biofilms and biocrystals. J. Nanosci. Nanotechnol., 6: 2209-2236. DOI: 10.1166/jnn.2006.502

Nicolini, C. and E. Pechkova, 2006b. Structure and growth of ultrasmall protein microcrystals by synchrotron radiation: I. μGISAXS and μdiffraction of P450scc. J. Cell. Biochem., 97: 544-552. DOI: 10.1002/jcb.20537

Nicolini, C., 1997. Protein-monolayer engineering: Principles and application to biocatalysis. Trends Biotechnol., 15: 395-401. DOI: 10.1016/S0167-7799(97)01084-6

Pechkova, E. and C. Nicolini, 2004. Protein nanocrystallography: A new approach to structural proteomics. Trends Biotechnol., 22: 117-122. DOI: 10.1016/j.tibtech.2004.01.011

Pechkova, E. and C. Nicolini, 2010. Domain organization and properties of LB lysozyme crystals down to submicron size. Anticancer Res., 30:2745-2748. PMID: 20683008

Pechkova, E. and C. Nicolini, 2011. In situ study of nanotemplate-induced growth of lysozyme microcrystals by submicron GISAXS. J. Synchrot. Radiat., 18: 287-292.

Pechkova, E., G. Tropriano, C. Riekel and C. Nicolini, 2004. Radiation stability of protein crystals grown by nanostructured templates: Synchrotron microfocus analysis. Spectrocheminica Acta B, 59: 1687-1693. DOI: 10.1016/j.sab.2004.07.020

Pechkova, E., G. Zanotti and C. Nicolini, 2003. Three-dimensional atomic structure of a catalytic subunit mutant of human protein kinase CK2. Acta Cryst. D, 59: 2133-2139. DOI: 10.1107/S0907444903018900

Pechkova, E., L. Belmonte, C. Riekel, D. Popovd and C. Koenige *et al.*, 2013. Laser-microdissection of protein crystals down to submicron dimensions. J. Nanomedicine Nanotechnol.

Pechkova, E., M. Sartore, L. Giacomelli and C. Nicolini, 2007. Atomic force microscopy of protein films and crystals. Rev. Scient. Instruments, 78: 093704-093704. PMID: 17902952

Pechkova, E., R. Gebhardt, C. Riekel and C. Nicolini, 2010. In situ μGISAXS: I. Experimental setup for submicron study of protein nucleation and growth. Biophys. J., 99: 1256-1261. DOI: 10.1016/j.bpj.2010.03.069

Pechkova, E., S. Tripathi, R.B.G. Ravelli, S. McSweeney and C. Nicolini, 2009. Radiation stability of proteinase K crystals grown by LB nanotemplate method. J. Struct. Biol., 168: 409-418. DOI: 10.1016/j.jsb.2009.08.005

Pechkova, E., V. Sivozhelezov, G. Tropiano, S. Fiordoro and C. Nicolini, 2005. Comparison of lysozyme structures derived from thin-film-based and classical crystals. Acta Cryst. D, 61: 803-808. DOI: 10.1107/S0907444905006578

Pechkova, E., V. Sivozhelezov, L. Belmonte and C. Nicolini, 2012a. Unique water distribution of Langmuir-blodgett versus classical crystals. J. Struct. Biol., 180: 57-64. DOI: 10.1016/j.jsb.2012.05.021

Pechkova, E., D. Scudieri, L. Belmonte and C. Nicolini, 2012b. Oxygen-bound hell's gate globin I by classical versus LB nanotemplate method. J. Cellular Biochem., 113: 2543-2548. DOI: 10.1002/jcb.24131

PyMol, 2012. The PyMOL Molecular Graphics System, Schrödinger, LLC. L. Schrödinger, editor. Schrödinger, LLC.

Riekel, C., M. Burghammer, R. Davies, R. Gebhardt and D. Popov, 2009. Fundaments of Soft Condensed Matter Scattering and Diffraction with Microfocus Techniques. In: Applications of Synchrotron Light to Scattering and Diffraction in Materials Life Sciences, Ezquerra, T.A., M. Garcia-Gutierrez, A. Nogales and M. Gomez (Eds.), Springer, Heidelberg, ISBN-10: 354095967X, pp: 91-104.

Santucci, S.C., D. Cojoc, H. Amenitsch, B. Marmiroli and B. Sartori *et al.*, 2011. Optical tweezers for synchrotron radiation probing of trapped biological and soft matter objects in aqueous environments. Analyt. Chem., 83: 4863-4870. DOI: 10.1021/ac200515x

Sayle, R.A., 1995. RASMOL: Biomolecular graphics for all. Trends Biochem. Sci., 20: 374-376. DOI: 10.1016/S0968-0004(00)89080-5

Vagin, A. and A. Teplyakov, 1997. MOLREP: An automated program for molecular replacement. J. Applied Cryst., 30: 1022-1025. DOI: 10.1107/S0021889897006766

ZEISS, 2012. Laser microdissection and optical tweezers. Zeiss.